

# Pseudogap at hot spots in the two-dimensional Hubbard model at weak coupling

Daniel Rohe and Walter Metzner

*Max Planck Institute for Solid State Research, D-70569 Stuttgart, Germany*

(Dated: June 19, 2018)

We analyze the interaction-induced renormalization of single-particle excitations in the two-dimensional Hubbard model at weak coupling using the Wick-ordered version of the functional renormalization group. The self energy is computed for real frequencies by integrating a flow equation with renormalized two-particle interactions. In the vicinity of hot spots, that is points where the Fermi surface intersects the umklapp surface, self energy effects beyond the usual quasi-particle renormalizations and damping occur near instabilities of the normal, metallic phase. Strongly enhanced renormalized interactions between particles at different hot spots generate a pronounced low-energy peak in the imaginary part of the self energy, leading to a pseudogap-like double-peak structure in the spectral function for single-particle excitations.

PACS: 71.10.Fd , 71.27.+a , 71.10.Hf

## I. INTRODUCTION

The most popular prototype model for the dynamics of electrons in the copper oxide planes of cuprate superconductors is the two-dimensional Hubbard model,<sup>1</sup> which captures two of the most prominent and universal features of these compounds: to be an antiferromagnetic Mott insulator at half filling and a d-wave superconductor at sufficiently strong doping. It is very difficult to compute the low-energy properties of the two-dimensional Hubbard model at strong coupling, as relevant to the cuprates. In fact, close to half filling the model exhibits complicated non-trivial behavior already at weak coupling, due to a mutual interplay of singularities in the particle-particle and particle-hole channel, which

cannot be captured by simple resummations of Feynman diagrams.

A systematic analysis of this interplay has been initiated in recent years with the development of functional renormalization group (fRG) methods for interacting Fermi systems.<sup>2</sup> The starting point of this approach is an exact hierarchy of differential flow equations for Green or vertex functions, which is obtained by differentiating the generating functional of the system with respect to an infrared cutoff  $\Lambda$  or some other energy scale. Approximations are then constructed by truncating this hierarchy and parametrizing the vertex functions with a manageable set of variables or functions. Already from the first fRG studies of the two-dimensional Hubbard model, which focussed on the flow of the two-particle vertex  $\Gamma$  and various susceptibilities in the one-loop approximation, a number of interesting conclusions could be drawn.<sup>3,4,5</sup> In particular, the expected existence of superconductivity with  $d_{x^2-y^2}$  symmetry was firmly established, at least at weak coupling. More importantly, it became clear that close to half filling correlations in the particle-particle and particle-hole channel are both strong and mutually influence each other.

The effect of correlations on single-particle excitations is seen most clearly in the self energy  $\Sigma(\mathbf{k}, \omega)$ , for frequencies  $\omega$  on the real axis. Zanchi<sup>6</sup> computed the flow of the frequency derivative of the self energy on the Fermi surface, which determines the wave function renormalization factor  $Z = [1 - \partial_\omega \text{Re}\Sigma(\mathbf{k}_F, \omega)|_{\omega=0}]^{-1}$ , for the special case of a half-filled Hubbard model with pure nearest neighbor hopping. In Fermi liquids  $Z$  yields the weight of the quasi-particle peak in the spectral function. Zanchi found that the  $Z$ -factor is strongly reduced when the renormalized vertex increases, the suppression being strongest near the van Hove points. Subsequently, Honerkamp and Salmhofer<sup>7</sup> computed the flow of the  $Z$ -factor for the two-dimensional Hubbard model at as well as away from half filling. While confirming an anisotropic reduction of  $Z$ , they observed that this suppression emerges much slower than the divergence of dominant interactions. In addition, they pointed out that the self energy does not significantly alter the vertex renormalization in the perturbative regime, that is before the interactions grow strongly. An fRG calculation of the imaginary part of the self energy at zero frequency,  $\text{Im}\Sigma(\mathbf{k}_F, 0)$ , was performed by Honerkamp.<sup>8</sup> In Fermi liquids this quantity is directly related to the decay rate of quasi-particles. For a hole-doped Hubbard model with a concave Fermi

surface that almost touches the van Hove points he found that  $\text{Im}\Sigma(\mathbf{k}_F, 0)$  is moderately anisotropic, with larger values for momenta closer the van Hove points. A closer look reveals that the imaginary part of the self energy is actually largest near a hot spot, foreshadowing already a main feature of our results presented below. The first fRG calculation of the full frequency dependence of the self energy has been performed very recently by Katanin and Kampf.<sup>9</sup> They computed the real and imaginary parts of  $\Sigma(\mathbf{k}_F, \omega)$  and the resulting spectral function  $A(\mathbf{k}_F, \omega)$  for the Hubbard model with nearest and next-to-nearest neighbor hopping at temperatures above  $T^*$  and observed the destruction of Fermi liquid behavior near  $T^*$  due to structures indicating the formation of a pseudogap, in particular for  $\mathbf{k}_F$  close to a van Hove point. For  $\mathbf{k}_F$  at short but finite distance from a van Hove point they found an additional peak between the two maxima that confine the pseudogap in the spectral function. Moving even further away from the van Hove point toward the diagonal of the Brillouin zone the three peaks gradually merge into one single peak.<sup>9</sup>

In this work we present a calculation of the full frequency dependence of the self energy and the resulting spectral function for the two-dimensional Hubbard model as obtained from the *Wick-ordered* version of the fRG.<sup>2,4</sup> This scheme has the advantage that only low-energy states contribute to the flow at low-energy scales, which leads to a better control of the necessary Fermi surface projections of momentum dependences compared to other fRG versions.<sup>7,8,9</sup> We do the calculation for frequencies directly on the real axis, thus avoiding analytical continuation. In agreement with previous studies we obtain marked deviations from Fermi liquid behavior for Fermi momenta near van Hove points, and also near other hot spots in the case of filling factors above the van Hove singularity: the imaginary part of the self energy develops a pronounced peak at low frequencies, which leads to a double-peak structure in the spectral function reminiscent of a pseudogap. This double peak gradually transforms into a single peak when moving away from the hot spot or van Hove regions, and also upon raising the temperature. Unlike Ref. 9 we never obtain a third peak in the pseudogap valley.

## II. MODEL

We consider the one-band Hubbard model defined by the Hamiltonian

$$H = \sum_{\mathbf{j}, \mathbf{j}'} \sum_{\sigma} t_{\mathbf{j}\mathbf{j}'} c_{\mathbf{j}\sigma}^{\dagger} c_{\mathbf{j}'\sigma} + U \sum_{\mathbf{j}} n_{\mathbf{j}\uparrow} n_{\mathbf{j}\downarrow}, \quad (1)$$

with a local repulsion  $U > 0$  and hopping amplitudes  $t_{\mathbf{j}\mathbf{j}'} = -t$  between nearest neighbors and  $t_{\mathbf{j}\mathbf{j}'} = -t'$  between next-to-nearest neighbors on a square lattice. The corresponding dispersion relation

$$\epsilon_{\mathbf{k}} = -2t(\cos k_x + \cos k_y) - 4t' \cos k_x \cos k_y \quad (2)$$

has saddle points at  $\mathbf{k} = (0, \pi)$  and  $(\pi, 0)$ , leading to logarithmic van Hove singularities in the non-interacting density of states at energy  $\epsilon_{\text{vH}} = 4t'$ .

## III. METHOD

We use the Wick-ordered version of the fRG as proposed by Salmhofer,<sup>2</sup> which has been concisely described and used in the context of an explicit one-loop computation of the two-particle vertex for the two-dimensional Hubbard model.<sup>4</sup> In this scheme, to second order in the two-particle vertex the flow of the self energy  $\Sigma^{\Lambda}$  is determined by a single two-loop Feynman diagram, shown in Fig. 1, and the flow of the two-particle vertex  $\Gamma^{\Lambda}$  is obtained to second order by evaluating the one-loop diagram in Fig. 1. The internal lines without slash in the Feynman diagrams correspond to the bare propagator

$$D^{\Lambda}(k) = \frac{\Theta(\Lambda - |\xi_{\mathbf{k}}|)}{ik_0 - \xi_{\mathbf{k}}}, \quad (3)$$

where  $\xi_{\mathbf{k}} = \epsilon_{\mathbf{k}} - \mu$  and  $\Lambda > 0$  is the cutoff; the slashed lines represent  $\partial_{\Lambda} D^{\Lambda}$ , which is proportional to  $\delta(\Lambda - |\xi_{\mathbf{k}}|)$ . Note that  $D^{\Lambda}$  has support only on a shell of energetic width  $\Lambda$  around the Fermi surface, that is for momenta  $\mathbf{k}$  with  $|\xi_{\mathbf{k}}|$  *below* scale  $\Lambda$ . A first order contribution to  $\Sigma^{\Lambda}$  (Hartree term) has been absorbed in a shift of the chemical potential, such that the leading contributions are quadratic in  $\Gamma^{\Lambda}$ . We note that in the full hierarchy of flow equations of the Wick-ordered fRG also one-particle reducible terms contribute.

However, these have to be considered only if the flow is computed beyond second order in  $\Gamma^\Lambda$ .

For a spin-rotationally invariant system the vertex is uniquely determined by two functions depending on momenta only, namely a singlet component  $\Gamma_s^\Lambda$  and a triplet component  $\Gamma_t^\Lambda$ , as described in Ref. 4. In the present work the vertex is defined with an extra factor 1/2 compared to the conventions in Ref. 4. The flow equation for the vertex can only be solved if the momentum and frequency dependence of the vertex is parametrized by a reduced set of variables. The frequency dependence of  $\Gamma^\Lambda$  can be neglected without much damage because it is absent in the bare interaction, and irrelevant in the sense of power counting in the limit  $\Lambda \rightarrow 0$ . The frequency integrals in the Feynman diagrams in Fig. 1 can then be carried out analytically. The resulting one-loop flow equations for  $\Gamma_s^\Lambda(\mathbf{k}', \mathbf{k}_2'; \mathbf{k}_1, \mathbf{k}_2)$  and  $\Gamma_t^\Lambda(\mathbf{k}', \mathbf{k}_2'; \mathbf{k}_1, \mathbf{k}_2)$  given in Ref. 4 are supplemented by the flow equation for the imaginary part of  $\Sigma^\Lambda(\mathbf{k}, \omega)$  for arbitrary real frequencies  $\omega$  given as

$$\begin{aligned} \partial_\Lambda \text{Im} \Sigma^\Lambda(\mathbf{k}, \omega) &= \pi \int \frac{d^2 \mathbf{p}}{(2\pi)^2} \int \frac{d^2 \mathbf{q}}{(2\pi)^2} \partial_\Lambda [\Theta(\Lambda - |\xi_{\mathbf{p}}|) \Theta(\Lambda - |\xi_{\mathbf{q}}|) \Theta(\Lambda - |\xi_{\mathbf{k}+\mathbf{q}-\mathbf{p}}|)] \\ &\times \{ [\Gamma_s^\Lambda(\mathbf{k}, \mathbf{q}; \mathbf{p}, \mathbf{k} + \mathbf{q} - \mathbf{p})]^2 + 3[\Gamma_t^\Lambda(\mathbf{k}, \mathbf{q}; \mathbf{p}, \mathbf{k} + \mathbf{q} - \mathbf{p})]^2 \} \\ &\times F(\mathbf{q}; \mathbf{p}, \mathbf{k} + \mathbf{q} - \mathbf{p}) \delta(\omega - \xi_{\mathbf{p}} + \xi_{\mathbf{q}} - \xi_{\mathbf{k}+\mathbf{q}-\mathbf{p}}) \end{aligned} \quad (4)$$

with the combination of Bose ( $b$ ) and Fermi ( $f$ ) functions

$$F(\mathbf{q}, \mathbf{p}, \mathbf{p}') = [f(\xi_{\mathbf{q}}) - f(\xi_{\mathbf{p}'})] [f(\xi_{\mathbf{p}}) + b(\xi_{\mathbf{q}} - \xi_{\mathbf{p}'})] . \quad (5)$$

In contrast to its appearance  $F$  is symmetric in  $\mathbf{p}$  and  $\mathbf{p}'$ . The real part of  $\Sigma^\Lambda$  can be determined from  $\text{Im} \Sigma^\Lambda$  via a Kramers-Kronig relation. The momentum dependence of the vertex is discretized similarly to previous fRG calculations<sup>3,4,5</sup> by dividing the Brillouin zone into patches as shown in Fig. 2. The shape of the patches accounts for the fact that the momentum dependence normal to the Fermi surface is irrelevant in the sense of power counting, in contrast to the tangential momentum dependence. The flow equations are integrated from  $\Lambda = \Lambda_0 = \max_{\mathbf{k}} |\xi_{\mathbf{k}}|$  to  $\Lambda = 0$ . The initial conditions are  $\Gamma_s^{\Lambda_0} = U$ ,  $\Gamma_t^{\Lambda_0} = 0$ , and  $\Sigma^{\Lambda_0} = 0$ . From the result for the self energy  $\Sigma^\Lambda$  for  $\Lambda \rightarrow 0$  we compute the

spectral function  $A(\mathbf{k}, \omega) = -2\text{Im}G(\mathbf{k}, \omega)$ . To avoid the computationally expensive self-consistent determination of the interacting Fermi surface, we remove Fermi surface shifts by subtracting  $\text{Re}\Sigma(\mathbf{k}_F, 0)$  from the self energy in the Dyson equation  $G^{-1} = G_0^{-1} - \Sigma$ .

#### IV. RESULTS

We focus on the two-dimensional Hubbard model with a negative next-to-nearest neighbor hopping amplitude  $t' = -0.1t$  and two different average densities,  $n = 0.92$  and  $n = 1$ , respectively. In both cases the Fermi surface given by  $\xi_{\mathbf{k}} = 0$  is closed around  $(\pi, \pi)$  and has finite curvature everywhere, see Fig. 2. In the following the so-called hot spots, that is the points where the Fermi surface intersects the umklapp surface, will play a special role. The momenta on the umklapp surface obey the relation  $\epsilon_{\mathbf{k}+\mathbf{Q}} = \epsilon_{\mathbf{k}}$  with  $\mathbf{Q} = (\pi, \pi)$ . For  $n = 0.92$  the Fermi surface almost touches the van Hove points, and the hot spots are very close to the latter. By contrast, for  $n = 1$  the hot spots are well separated from the van Hove points. We set  $t = 1$ , that is all energies are given in units of  $t$ . We fix a low finite temperature  $T = 0.05$  and choose the bare interaction  $U$  such that the couplings flow to strong values but do not diverge for  $\Lambda \rightarrow 0$ . In other words, the temperature  $T$  is slightly above the scale  $T^*$  at which the one-loop flow diverges.

The complete frequency dependence of the imaginary part of the self energy  $\text{Im}\Sigma(\mathbf{k}_F, \omega)$  for high and low energies is shown in Fig. 3, for  $n = 0.92$  and a Fermi momentum  $\mathbf{k}_F$  which coincides with a hot spot. The fRG result is compared to the result from standard second order perturbation theory, which is obtained from the flow equation (4) when the renormalized vertex  $\Gamma^\Lambda$  is replaced by the bare interaction. While the vertex renormalization has virtually no influence on the self energy at high frequencies, it leads to a pronounced peak in  $\text{Im}\Sigma$  at low frequencies, which is absent in perturbation theory.

We now focus on the low-energy behavior. In Fig. 4 we plot  $\Sigma(\mathbf{k}_F, \omega)$  at small frequencies for  $n = 0.92$  and six different Fermi momenta  $\mathbf{k}_F$  situated in patches  $1, 2, \dots, 6$ , respectively. We show two different fRG results: in one case the bare interaction  $U$  has been tuned such that the renormalized vertex reaches a peak value  $\Gamma_{\text{max}}^{\Lambda=0} = 15$ , in the other  $\Gamma_{\text{max}}^{\Lambda=0} = 150$ . If the peak in  $\text{Im}\Sigma(\mathbf{k}_F, \omega)$  observed already in Fig. 3 is sufficiently strong,

it causes a sign change in the slope of  $\text{Re}\Sigma(\mathbf{k}_F, \omega)$  at small  $\omega$ . For  $\partial_\omega \text{Re}\Sigma(\mathbf{k}_F, \omega)|_{\omega=0} > 1$  this leads to a double-peak structure reminiscent of a pseudogap in the spectral function  $A(\mathbf{k}_F, \omega)$ , shown in Fig. 5. For a less strongly renormalized vertex, as well as for momenta away from the hot spot, the peak in  $\text{Im}\Sigma(\mathbf{k}_F, \omega)$  disappears gradually. As a consequence, the double peak in the spectral function is well developed only for  $\mathbf{k}_F$  near the hot spot, and for a comparatively large renormalized vertex, that is for  $T$  rather close to  $T^*$ . Otherwise, the self energy merely leads to an angle-dependent lifetime broadening of the quasi-particle peak in  $A(\mathbf{k}_F, \omega)$ .

For electron density  $n = 1$  the hot spot is situated in the third patch (see Fig. 2). Results for  $\Sigma(\mathbf{k}_F, \omega)$  and  $A(\mathbf{k}_F, \omega)$  are shown in Figs. 6 and 7, respectively. The fRG again yields a peak in  $\text{Im}\Sigma(\mathbf{k}_F, \omega)$  around  $\omega = 0$  for a hot spot momentum  $\mathbf{k}_F$ , but only for  $\Gamma_{\text{max}}^\Lambda = 150$ . Moreover, its absolute value is much smaller compared to the case  $n = 0.92$ , and it is less pronounced. Consequently, the corresponding spectral function exhibits only a mild dip. For weaker interactions or  $\mathbf{k}_F$  away from the hot spot  $A(\mathbf{k}_F, \omega)$  has a more or less conventional shape, with a single lifetime-broadened peak. This broadening is larger for momenta next to the hot spot, since the low-frequency part of  $\text{Im}\Sigma(\mathbf{k}_F, \omega)$  is still strongly enhanced, albeit not peaked, in these regions.

Note that there is nothing special about the density  $n = 1$  (half-filling) at weak coupling if  $t' \neq 0$ , in contrast to the case of strong coupling, for which the half-filled Hubbard model becomes a Mott insulator, and in contrast to the special case with pure nearest neighbor hopping ( $t' = 0$ ), for which the Fermi surface coincides with the umklapp surface at half-filling. The fact that the anomaly we observe in the self energy is more pronounced for a Fermi surface close to van Hove filling reflects the relevance of the van Hove singularities in the weak coupling limit.

To understand the mechanism behind the low-energy singularity in  $\text{Im}\Sigma(\mathbf{k}, \omega)$  for hot spot momenta  $\mathbf{k}_{\text{hs}}$ , we consider the flow eq. (4) in the limit  $T \rightarrow 0$  and  $\omega \rightarrow 0$ . At  $T = 0$  the function  $F(\mathbf{q}, \mathbf{p}, \mathbf{p}')$  reduces to a step function which constrains the relative signs of

$\xi_{\mathbf{q}}$ ,  $\xi_{\mathbf{p}}$ , and  $\xi_{\mathbf{p}'}$ :

$$F(\mathbf{q}, \mathbf{p}, \mathbf{p}') = \begin{cases} -1 & \text{for } \xi_{\mathbf{q}} < 0; \xi_{\mathbf{p}}, \xi_{\mathbf{p}'} > 0 \\ -1 & \text{for } \xi_{\mathbf{q}} > 0; \xi_{\mathbf{p}}, \xi_{\mathbf{p}'} < 0 \\ 0 & \text{else} \end{cases} \quad (6)$$

Energy conservation imposed by the  $\delta$ -function in Eq. (4) then implies that in the limit  $\omega \rightarrow 0$  the internal momenta  $\mathbf{q}$ ,  $\mathbf{p}$ ,  $\mathbf{p}' = \mathbf{k} + \mathbf{q} - \mathbf{p}$  are all constrained to the Fermi surface. If in addition  $\mathbf{k}$  is a Fermi momentum, all ingoing and outgoing momenta of  $\Gamma^\Lambda$  in Eq. (4) have to lie on the Fermi surface. At low finite  $T$  or  $\omega$  this constraint is slightly relaxed such that the internal momenta can be taken from a thin shell of energetic width of order  $T$  or  $\omega$  around the Fermi surface. Since one of the internal momenta  $\mathbf{p}$  on the right hand side of the flow equation is forced to sit at scale  $|\xi_{\mathbf{p}}| = \Lambda$  by the  $\Lambda$ -derivative of the cutoff functions, the flow of  $\text{Im}\Sigma^\Lambda$  receives sizable contributions only when  $\Lambda$  has reached the scale  $T$  or  $\omega$ . In two dimensions there are two generic types of momentum-conserving interaction processes with all ingoing  $(\mathbf{k}_1, \mathbf{k}_2)$  and outgoing  $(\mathbf{k}'_1, \mathbf{k}'_2)$  momenta on the Fermi surface: forward scattering processes  $(\mathbf{k}'_1 = \mathbf{k}_1 \text{ or } \mathbf{k}'_1 = \mathbf{k}_2)$  and Cooper processes  $(\mathbf{k}_2 = -\mathbf{k}_1)$ . In lattice systems also certain umklapp processes in which a reciprocal lattice vector is added to the total momentum can fulfill this condition. They can play an important role, as discussed below.

Looking at the renormalized interactions obtained from the one-loop flow of  $\Gamma^\Lambda$  for our two choices of densities,  $n = 0.92$  and  $n = 1$ , we find that in both cases the dominant effective interactions are in the spin singlet channel with ingoing and outgoing momenta near hot spots. Among these, interactions with a momentum transfer  $\mathbf{Q} = (\pi, \pi)$  are leading. For  $n = 0.92$  the vertex is maximal for the scattering of a Cooper pair with both partners on hot spots to two other hot spots with a momentum transfer  $\mathbf{Q}$ , that is  $(\mathbf{k}_{\text{hs}}, -\mathbf{k}_{\text{hs}}) \mapsto (\mathbf{k}'_{\text{hs}}, -\mathbf{k}'_{\text{hs}})$  with  $\mathbf{k}'_{\text{hs}} - \mathbf{k}_{\text{hs}} = \mathbf{Q}$ . Combined Cooper and forward scattering processes  $(\mathbf{k}_{\text{hs}}, -\mathbf{k}_{\text{hs}}) \mapsto (\mathbf{k}_{\text{hs}}, -\mathbf{k}_{\text{hs}})$  are also among the strongly enhanced interactions at that density. Computing the contributions to  $\text{Im}\Sigma$  from different scattering processes separately reveals that the peak at hot spots is indeed generated mostly by Cooper and  $\mathbf{Q}$ -transferring interactions, where the latter are slightly more important. For  $n = 1$  the leading interaction is an umklapp process,  $(\mathbf{k}_{\text{hs}}, \mathbf{k}_{\text{hs}}) \mapsto (\mathbf{k}'_{\text{hs}}, \mathbf{k}'_{\text{hs}})$  with  $\mathbf{k}'_{\text{hs}} - \mathbf{k}_{\text{hs}} = \mathbf{Q}$ ,



closely followed by a  $\mathbf{Q}$ -transferring Cooper process on hot spots. However, the total contribution from Cooper processes (including the  $\mathbf{Q}$ -transferring one) to the peak in  $\text{Im}\Sigma$  is very small compared to the total contribution from  $\mathbf{Q}$ -transferring processes in that case. The importance of  $\mathbf{Q}$ -transferring and Cooper interactions in the two-dimensional Hubbard model is well known from earlier fRG and other studies, and reflects strong antiferromagnetic and superconducting correlations, respectively.

The above mechanism for the destruction of fermionic quasi-particles close to the Fermi surface is completely different from the mechanism leading to Luttinger liquid behavior in one-dimensional electron systems.<sup>11</sup> In one-dimensional (gapless) electron liquids the renormalized interactions remain finite, while the self-energy receives nevertheless enhanced contributions at low energy due to a large phase space for scattering processes. However,  $\text{Im}\Sigma(k_F, \omega)$  does not develop a peak at  $\omega = 0$ , it just vanishes much slower for  $T \rightarrow 0, \omega \rightarrow 0$  than in a Fermi liquid. At  $T = 0$ , one obtains  $\text{Im}\Sigma(k_F, \omega) \propto |\omega|^{1-\eta}$ , where  $\eta$  is a positive exponent which is relatively small for systems with short-range interactions. The spectral function  $A(k, \omega)$  exhibits a single peak centered at  $\omega = 0$  for  $k = k_F$ , and a split peak at finite energy for  $k$  away from the Fermi point.<sup>12</sup> This peak splitting is not related to pseudogap behavior, it is rather due to spin-charge separation. Applying our fRG scheme to a one-dimensional Luttinger liquid system at weak coupling yields finite renormalized interactions, due to a well-known cancellation of singularities in the particle-particle and particle-hole channel. For the self-energy as computed from the flow equation (4) in one dimension this implies a linear frequency dependence,  $\text{Im}\Sigma(k_F, \omega) \propto |\omega|$ , yielding a single broadened peak in  $A(k_F, \omega)$  as expected, but missing the anomalous exponent  $\eta$ . The latter could be captured by feeding the self-energy back on the right hand side of its flow equation, most simply via a wave function renormalization, as described for the one-particle irreducible fRG in Ref. 7. The situation is different if umklapp scattering (so-called  $g_3$ -terms) are relevant, as in the one-dimensional Hubbard model at half-filling. In that case renormalized interactions grow strong and a charge gap opens, leading to a gap in the spectral function  $A(k_F, \omega)$ , which is clearly signalled by a suppression of spectral weight at low frequencies within the fRG scheme.

Our results agree only partially with those obtained by Katanin and Kampf,<sup>9</sup> who

computed the full frequency dependence of the self energy from the one-particle irreducible version of the fRG,<sup>10</sup> with a truncation of the exact hierarchy of flow equations at the same order as in our calculation. For a Fermi momentum very close to a van Hove point they obtained a single peak in  $\text{Im}\Sigma$  resulting in a double peak in the spectral function, in agreement with our calculation. However, for Fermi momenta at some moderate distance from the van Hove point they found a double peak in  $\text{Im}\Sigma$  leading to a three-peak structure in the spectral function, which we do not observe in our results. In both approaches, Wick-ordered as well as one-particle irreducible fRG, the peaks in  $\text{Im}\Sigma$  are generated by strongly enhanced effective interactions, and are thus most pronounced at temperatures close to the instability scale  $T^*$ . The different structure of  $\text{Im}\Sigma$  obtained from the two fRG versions can be traced back to a different division of momentum integrals in high and low energy modes. In both cases the energy variable  $\omega$  is related to the excitation energies on internal lines:  $\omega = \xi_{\mathbf{p}} + \xi_{\mathbf{p}'} - \xi_{\mathbf{q}}$ . In the Wick-ordered scheme all excitation energies are at or below the cutoff, that is  $|\xi| \leq \Lambda$ . As a consequence, the flow for  $\text{Im}\Sigma^\Lambda(\mathbf{k}, \omega)$  with  $|\omega| > 0$  stops completely for  $\Lambda < |\omega|/3$ . In a situation where the vertex  $\Gamma^\Lambda$  grows strongly at very small scales,  $\Lambda \rightarrow 0$ , the imaginary part of the self energy therefore receives the corresponding large contributions only for small frequencies, which leads necessarily to a single peak with maximal height at  $\omega = 0$ . By contrast, in the two-loop diagram generating the flow of  $\text{Im}\Sigma^\Lambda$  in the one-particle irreducible scheme one excitation energy is at scale  $\Lambda$ , the second at a scale  $\Lambda' > \Lambda$ , and the third one *above* the scale  $\Lambda'$ , where  $\Lambda'$  is the scale of the vertex  $\Gamma^{\Lambda'}$  in the diagram. Note that the two-loop diagram for the self energy in the one-particle irreducible fRG is non-local in the cutoff. The crucial point is that not all excitation energies are bounded by the cutoff. Therefore, the flow of  $\text{Im}\Sigma^\Lambda(\mathbf{k}, \omega)$  does not stop for  $\Lambda \ll |\omega|$ , and the strong enhancement of  $\Gamma^{\Lambda'}$  for  $\Lambda' \rightarrow 0$  does not necessarily enhance  $\text{Im}\Sigma^\Lambda(\mathbf{k}, \omega)$  most strongly for the smallest energies. However, to obtain a double peak in  $\text{Im}\Sigma$  with maxima at finite frequencies, say  $\omega_\pm$ , the contribution with at least one excitation energy of order  $\omega_\pm$  must be particularly large. This is possible only if the vertex is not enhanced most strongly for cases with all ingoing and outgoing momenta on the Fermi surface, but rather for some interaction processes with at least one momentum away from the Fermi surface. One should also keep in mind

that contributions from momenta away from the Fermi surface might be overestimated in the one-particle irreducible fRG with a momentum discretization by patches, since the dependence of the vertex  $\Gamma^\Lambda$  normal to the Fermi surface is weak only within a shell  $|\xi_{\mathbf{k}}| < \Lambda$  in momentum space.

We finally note that the  $Z$ -factor defined as  $Z = [1 - \partial_\omega \text{Re}\Sigma(\mathbf{k}_F, \omega)|_{\omega=0}]^{-1}$  does not provide sufficient information to parametrize the low-frequency dependence of the self energy, if the imaginary part develops a low-energy peak. Furthermore,  $Z$  does not provide any information on the low-energy weight in the spectral function in that case. Since the slope of  $\text{Re}\Sigma$  becomes positive near the hot spots, the  $Z$ -factor does not even satisfy the inequality  $0 < Z \leq 1$ .

## V. CONCLUSION

In summary, we have presented a weak-coupling calculation of the self energy  $\Sigma(\mathbf{k}, \omega)$  for the two-dimensional Hubbard model with a renormalization of effective interactions which fully treats the interplay of particle-particle and particle-hole channels. Strong renormalizations of single-particle excitations via self energy effects were observed for momenta near hot spots on the Fermi surface, if the system is close to an instability where the renormalized interactions are strongly enhanced. In this case the quasi-particle peak in the spectral function  $A(\mathbf{k}, \omega)$  is replaced by a double-peak structure reminiscent of a pseudogap. Further more, the fRG flow enables us to identify the correlations which are responsible for this feature, and thus offers substantial insight into the underlying microscopic mechanism. Evidently, the perturbative truncation of the flow equations becomes more and more uncontrolled in the regime of large renormalized interactions. We can thus only conclude that single-particle excitations near hot spots are strongly affected by interactions, but higher order contributions to the self energy are expected to become important at a certain point.

The tendency to pseudogap formation found in the above weak-coupling calculation is restricted to a narrow temperature scale and also to a narrow regime in momentum space, namely close to the hot spots. In contrast, the pseudogap phenomena in hole-doped

cuprate superconductors<sup>13</sup> are observed in a much wider temperature range, and are seen almost everywhere on the Fermi surface. This is undoubtedly due to the fact that the interaction in these materials is strong. Indeed, numerical results for the two-dimensional Hubbard model at large  $U$  obtained from quantum cluster approaches<sup>14</sup> provide evidence for extended pseudogap behavior near half-filling.

Our observation that for moderate interaction strength the pseudogap formation is favored at hot spots is in accordance with recent results obtained by Kyung et al.<sup>15</sup> on the basis of the two-particle self-consistent (TPSC) approach, as well as with the findings by S  n  chal and Tremblay<sup>16</sup> from cluster perturbation theory. In both references the focus is put on electron-doped cuprate superconductors, and it is argued that these compounds may be more weakly coupled at optimal doping, as opposed to the hole-doped materials. Therefore, it seems more appropriate to compare our results with experimental data on electron-doped cuprates. Note that at weak coupling the dominant correlations are strongly affected by the the Fermi surface topology and its intersection with the umklapp surface, while no qualitative changes occur at the transition from electron to hole-doped fillings. Hence, we may discuss qualitative properties of electron-doped cuprates, although we computed for densities  $n \leq 1$ . Unfortunately, the angular-resolved photoemission (ARPES) data for electron-doped cuprates available to this day are controversial. Very recently Claesson et al.<sup>17</sup> have presented measurements which do not show any signs of pseudogap behaviour, or other fingerprints of strong correlations in the  $(\pi, \pi)$ -transferring channel. On the other hand, earlier observations by Armitage et al.<sup>18</sup> are indeed partially consistent with our results. There, in a certain parameter range the Fermi surface vanishes around the hot spots where it would intersect the umklapp surface, and single-particle spectral weight is shifted to lower energies in that region. However, in these samples the qualitative picture changes as a function of doping. For a heavily underdoped system small electron pockets appear near  $(\pi, 0)$ , while the remaining part of the would-be Fermi surface is destroyed, also along the zone diagonal. Toyama and Maekawa<sup>19</sup> argue from calculations on a  $t - t' - t'' - J$  model that this may be due to the closeness to the antiferromagnetic phase, which is not as easily destroyed by doping as it is for hole-doped cuprates. Alternatively, this feature can be due to a small change in the

repulsive interaction as a function of doping, as suggested in reference 15. In both cases the interaction needs to be sufficiently large, and is outside the weakly coupled regime.

A comprehensive understanding of cuprate superconductors and other strongly correlated electron systems is still hampered by a lack of theoretical methods and frequently also by difficulties in obtaining reliable experimental data. At the present stage of its development the fRG can contribute by offering a controlled and transparent treatment of electron correlations at weak coupling. This captures already a variety of non-trivial phenomena, but misses genuine strong coupling physics, such as the Mott transition. In the long run one may envisage combining strong coupling methods for short range correlations with fRG schemes for the long range part.

**Acknowledgements:** We are grateful to C. Honerkamp, A. Katanin, D. Manske, and M. Salmhofer for valuable discussions. This work has been supported by the DFG Grant No. Me 1255/6-1.

- 
- <sup>1</sup> P.W. Anderson, *Science* **235**, 1196 (1987).
  - <sup>2</sup> M. Salmhofer, *Renormalization* (Springer, Berlin, 1998).
  - <sup>3</sup> D. Zanchi and H.J. Schulz, *Phys. Rev. B* **54**, 9509 (1996); *ibid* **61**, 13609 (2000).
  - <sup>4</sup> C.J. Halboth and W. Metzner, *Phys. Rev. B* **61**, 7364 (2000); *Phys. Rev. Lett.* **85**, 5162 (2000).
  - <sup>5</sup> C. Honerkamp et al., *Phys. Rev. B* **63**, 035109 (2001).
  - <sup>6</sup> D. Zanchi, *Europhys. Lett.* **55**, 376 (2001).
  - <sup>7</sup> C. Honerkamp and M. Salmhofer, *Phys. Rev. B* **67**, 174504 (2003).
  - <sup>8</sup> C. Honerkamp, *Eur. Phys. J. B* **21**, 81 (2001).
  - <sup>9</sup> A.A. Katanin and A.P. Kampf, *Phys. Rev. Lett.* **93**, 106406 (2004)
  - <sup>10</sup> M. Salmhofer and C. Honerkamp, *Prog. Theor. Phys.* **105**, 1 (2001).
  - <sup>11</sup> T. Giamarchi, *Quantum Physics in One Dimension* (Oxford University Press, New York,

- 2003).
- <sup>12</sup> V. Meden and K. Schönhammer, Phys. Rev. B **46**, 15753 (1992); J. Voit, Phys. Rev. B **47**, 6740 (1993).
  - <sup>13</sup> For a review on the pseudogap in High- $T_c$  cuprates, see T. Timusk and B. Statt, Rep. Prog. Phys. **62**, 61 (1999).
  - <sup>14</sup> For a review, see T. Maier, M. Jarrell, T. Pruschke, and M. Hettler, cond-mat/0404055.
  - <sup>15</sup> B. Kyung, J.-S. Landry, and A.-M.S. Tremblay, Phys. Rev. B **68**, 174502 (2003).
  - <sup>16</sup> D. Sénéchal and A.-M.S. Tremblay, Phys. Rev. Lett. **92**, 126401 (2004).
  - <sup>17</sup> T. Claesson et al., Phys. Rev. Lett. **93**, 136402 (2004)
  - <sup>18</sup> N.P. Armitage et al., Phys. Rev. Lett. **88**, 257001 (2002); Phys. Rev. Lett. **87**, 147003 (2001).
  - <sup>19</sup> T. Tohyama and S. Maekawa, Phys. Rev. B **64**, 212505 (2001)

$$\partial_\Lambda \text{---} \textcircled{\Sigma} \text{---} = \text{---} \textcircled{\Gamma} \text{---} \text{---} \textcircled{\Gamma} \text{---}$$

$$\partial_\Lambda \textcircled{\Gamma} = \textcircled{\Gamma} \text{---} \textcircled{\Gamma}$$

FIG. 1: Flow equations for the self energy  $\Sigma^\Lambda$  and the two-particle vertex  $\Gamma^\Lambda$ , respectively; the internal lines without slash correspond to the bare propagator  $D^\Lambda$ , the lines with a slash to its  $\Lambda$ -derivative  $\partial_\Lambda D^\Lambda$ .

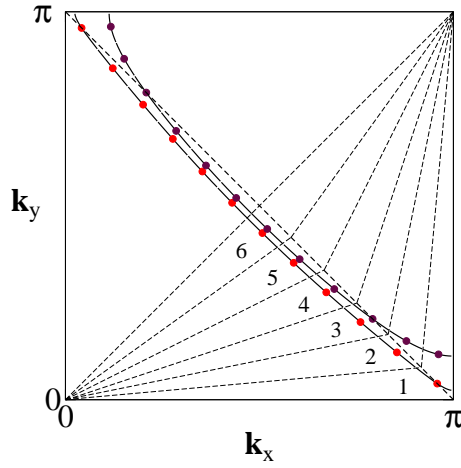


FIG. 2: Fermi surfaces (solid lines) for  $n = 0.92$  and  $n = 1$  in the first quarter of the Brillouin zone, Fermi points used for the discretization of momentum dependences, and the first 6 momentum space patches (confined by broken lines from  $(0, 0)$  to  $(\pi, \pi)$ ). The umklapp surface (broken line from  $(0, \pi)$  to  $(\pi, 0)$ ) intersects the Fermi surface at the so-called hotspots.

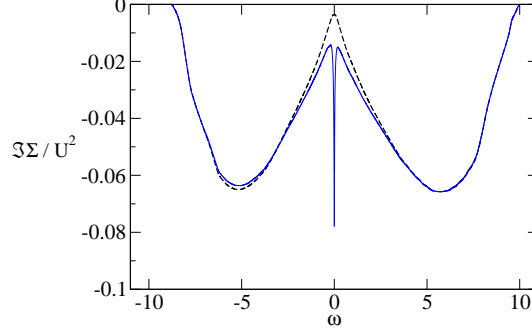


FIG. 3: Imaginary part of the self energy  $\text{Im}\Sigma(\mathbf{k}_F, \omega)$  normalized by  $U^2$  as a function of  $\omega$  for  $n = 0.92$  and  $\mathbf{k}_F$  on the hot spot (patch 1, see Fig. 2). The result from the fRG (blue solid line) is compared to the result from second order perturbation theory (black dashed line).

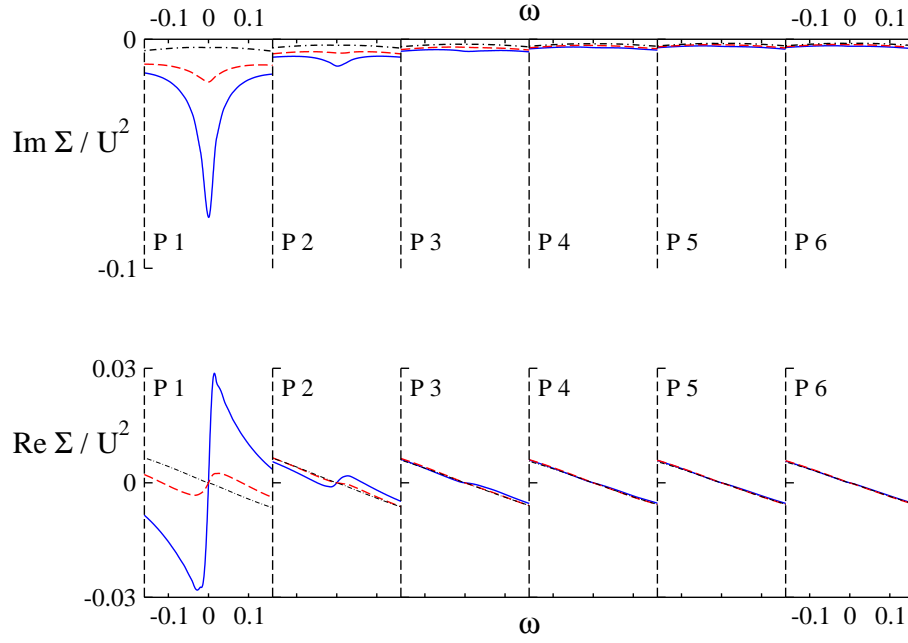


FIG. 4:  $\Sigma(\mathbf{k}_F, \omega)$  normalized by  $U^2$  at low energies  $\omega$  for  $n = 0.92$  and  $\mathbf{k}_F$  in patches  $1, 2, \dots, 6$ . Two results from the fRG with  $\Gamma_{\text{max}}^\Lambda = 150$  (blue solid lines) and  $\Gamma_{\text{max}}^\Lambda = 15$  (red dashed lines) are compared to each other; the former is obtained by choosing  $U = 1.815$ , the latter for  $U = 1.685$ . The results from second order perturbation theory for  $U = 1.815$  (black dash-dotted lines) are also shown for comparison.



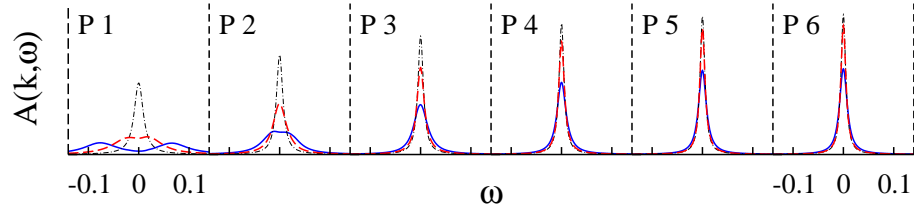


FIG. 5: Spectral function  $A(\mathbf{k}_F, \omega)$  at small frequencies  $\omega$  as obtained from the self energy results presented in Fig. 4.

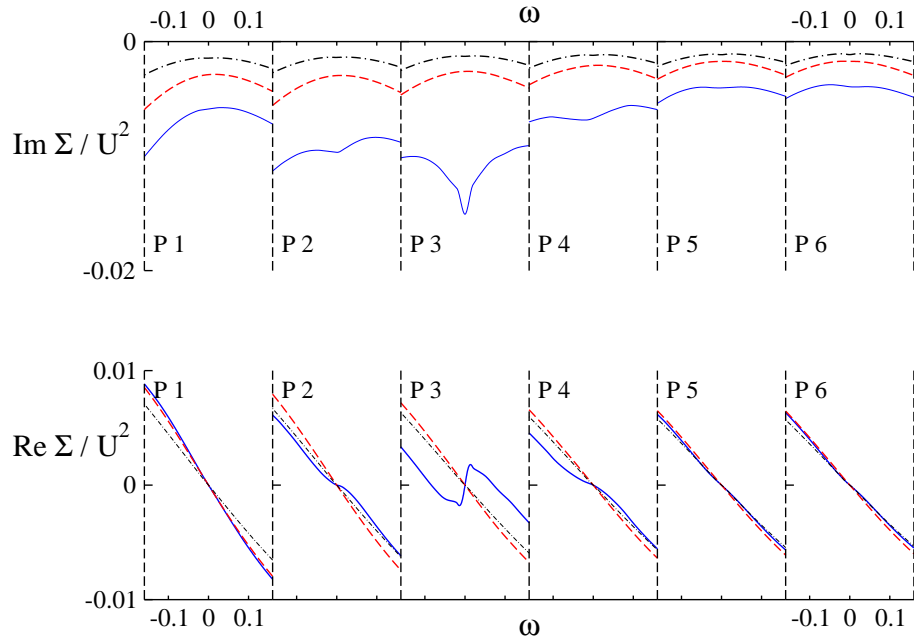


FIG. 6:  $\Sigma(\mathbf{k}_F, \omega)$  as in Fig. 4 but for  $n = 1$ .

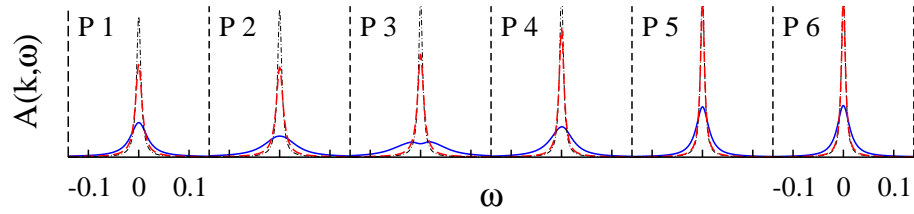


FIG. 7: Spectral function as in Fig. 5 but for  $n = 1$ .